American Mineralogist, Volume 62, pages 36–50, 1977

Vibrational spectra of the alkaline earth double carbonates

BARRY E. SCHEETZ AND WILLIAM B. WHITE

Materials Research Laboratory and Department of Geosciences
The Pennsylvania State University, University Park, Pennsylvania 16802

Abstract

Raman spectra and mid-range and far infrared spectra have been measured on polycrystalline norsethite [$BaMg(CO_3)_2$], barytocalcite [$BaCa(CO_3)_2$], the high-temperature modification of barytocalcite, huntite [$CaMg_3(CO_3)_4$], benstonite [$Ca_7Ba_6(CO_3)_{13}$], and alstonite [$CaBa(CO_3)_2$]. Factor-group calculations permit the assignment of the internal modes of the known structures. Effects of ordering in these derivative structures appear mainly in the IR spectra. A degree of translational disorder in the high-temperature modification of barytocalcite and in alstonite appears as a line broadening of the symmetric stretching mode in the Raman spectra.

Introduction

Seven known minerals containing alkaline-earth cations possess derivative or superstructures based on the calcite or aragonite structures (Table 1).

Two distinct types of ordering occur in the double carbonates. The first type represents an ordering of cation layers, while the second type is based on a superstructure of calcite with an ordering of cations within the layers. The high-temperature barytocalcite, barytocalcite, norsethite, and dolomite belong to the first type, and benstonite and huntite belong to the second type.

Barytocalcite (Dickens and Bowen, 1971) has a monoclinic cell, with space group $P2_1/m$ and $Z = 2$, that is related to the rhombohedral cell of calcite. If one considers Ca and Ba as identical, then a pseudocell can be constructed along the monoclinic $\{10\bar{1}\}_{mono} = a_{pc}$; $\{010\}_{mono} = b_{pc}$; and $\{101\}_{mono} = c_{pc}$. The pseudocell matches well with the orthohexagonal cell of calcite. The barytocalcite cell possesses alternating layers of Ca and Ba ions and two non-equivalent carbonate ions, one associated with the Ba ion and one with the Ca ion. The carbonate groups are non-planar and rotated 30° about "3-fold axis" with respect to the calcite carbonate groups. In addition, the carbonate group related to the calcium layer is tilted by 20° with respect to (101). Perpendicular to the layering, barytocalcite possesses a three-layer repeat similar to calcite, but because of the 30° rotation of the carbonate groups, the structure in this respect is similar to aragonite.

Prior to the structural determination of Dickens and Bowen (1971), Alm (1960) had investigated the structure and determined the space group to be $P2_1$. A second-harmonic generation test performed on a specimen verified the centrosymmetric cell and supports Dickens and Bowen's assignment of space group $P2_1/m$.

Norsethite (Lippmann, 1973) has a cell (space group $R32$) similar to dolomite, with alternating $Mg–CO_3–Ba–CO_3$ layers. In norsethite, however, the planar carbonate groups are rotated by 17.5° about the "3-fold axis" with respect to calcite, and the carbonate ions follow a fundamentally different stacking pattern than in dolomite. The carbonate groups in norsethite are related by two fold axes, while in dolomite they are related by a center of symmetry.

The second type of ordering includes ordered cation sites within the cation layers. Of the two examples studied, only the structure of huntite is known in detail (Graf and Bradley, 1962). Huntite is related to calcite by $a_{hex} = 9.505 = 2 \times 4.752$; $c_{hex} = 7.821 = 15.642/2$. The relationship to calcite arises from the ordering of the cations on the expanded cation layer (Fig. 1). Two crystallographically distinct carbonate groups are present—one in the basal plane of the cell and three symmetry-related CO_3^{2-} canted to the basal plane.

No detailed structural data are available for benstonite, which possesses a superstructure of calcite, or for alstonite, an aragonite-related, polymorphic

Table 1. Crystallographic data on alkaline earth double carbonate minerals

Mineral	Formula	Space Group	Cell Constants (Å)	Site Symmetry of Carbonate Ion	Reference of Structural Determination
Dolomite	$CaMg(CO_3)_2$	$R\bar{3}$	$a_{hex} = 4.8079$ $c_{hex} = 16.010$	$2CO_3(1)$-C_3	Graf (1961)
Huntite	$CaMg_3(CO_3)_4$	R32	$a_{hex} = 9.505$ $c_{hex} = 7.821$	$CO_3(1)$-D_3 $3CO_3(2)$-C_2	Graf and Bradley (1962)
Norsethite	$MgBa(CO_3)_2$	R32	$a_{hex} = 5.017$ $c_{hex} = 16.77$	$2CO_3(1)$-C_3	Mrose et al. (1961)
Barytocalcite	$CaBa(CO_3)_2$	$P2_1/m$	$a_o = 8.134$ $b_o = 5.229$ $c_o = 6.547$ $\beta_o = 106°02'$	$2CO_3(1)$-C_s $2CO_3(2)$-C_s	Dickens and Bowen (1971)
Alstonite	$CaBa(CO_3)_2$	Pmcn	$a_o = 4.99$ $b_o = 8.77$ $c_o = 6.11$	Unknown	
Benstonite	$Ca_7Ba_6(CO_3)_{13}$	$R\bar{3}$	$a_{hex} = 18.28$ $c_{hex} = 8.67$	Unknown	

phase of barytocalcite. Alstonite is claimed to be triclinic, with a large superstructure cell (Sartori, 1975). The structure of the high-temperature form of barytocalcite is unknown except that it is trigonal with the lattice parameters listed in Table 1 (Chang, 1965).

Research on the vibrational spectra of the carbonate minerals through 1973 was reviewed by White (1974a). Of particular note is the work of Adler and Kerr (1963), who interpreted the mid-range infrared spectra of many double carbonates in terms of site distortions and non-equivalent carbonate ions. More recently Raman spectra have been published on other calcite-structure carbonates (Rutt and Nicola, 1974), but no Raman data on the double carbonates have appeared. Rossman and Squires (1974) published an infrared spectrum of alstonite and spectra of the ν_4 band of barytocalcite and benstonite. Yamamoto *et al.* (1975) have made a very careful analysis of the vibrational spectrum of dolomite.

Experimental

Samples for this investigation were as far as possible obtained from their type localities. In a few cases, the samples have been subjects of previous scientific studies and hence their value as documented specimens (Table 2).

Norsethite was precipitated as the primary phase in Hood and Steidl's (1973) procedure for the preparation of benstonite. The norsethite was characterized by X-ray diffraction and purified by heavy-liquid separation.

Chang (1965) has shown that at 525°C barytocalcite undergoes a phase transition to what he refers to as a disordered calcite-like structure. A sample of barytocalcite from the type locality was sealed under vacuum in a quartz ampule, heated to 670°C for 96 hours, and then water-quenched. The resulting X-ray diffraction pattern was indexed on a rhombohedral cell with space-group symmetry *R*32. This transition is reversible as shown by DTA. The experimental value for the phase transition was 525°C, in agreement with Chang's result, also 525°C.

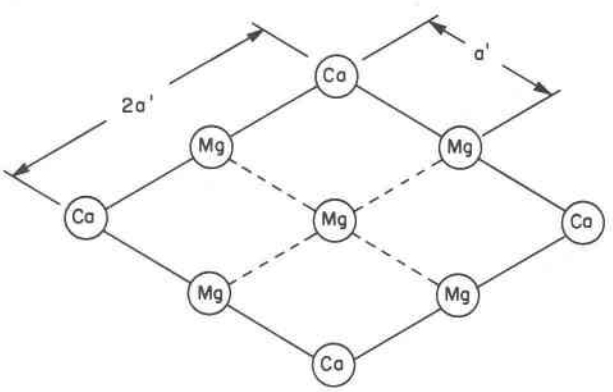

Fig. 1. Ordering of the cation layer in huntite, $CaMg_3(CO_3)_4$. Adapted from Lippmann (1973).

Table 2. Localities of natural double carbonates

Mineral	Formula	Location	Source	Description
Huntite	$CaMg_3(CO_3)_4$	Current Creek, NV	D. L. Graf (U. of Illinois)	White powder
		Tea Creek, Australia	D. L. Graf (U. of Illinois)	White powder
		Wind Cave, SD	(Authors Collection)	White powder
Barytocalcite	$CaBa(CO_3)_2$	Alston Moor, England	R. W. Grant (Lafayette College)	Single crystal LC #4473
		Blaygill, Alston, England	(Authors Collection)	Massive with single crystals
		Cambridge, England	Genth Collection	Single crystals
Alstonite	$CaBa(CO_3)_2$	Moore Hill, England	R. W. Grant (Lafayette College)	Twinned single crystals LC #4470
		Alston Moor, England	L. L. Y Chang (Miami U.)	Massive with single crystals
Benstonite	$Ca_7Ba_6(CO_3)_{13}$	Minerva Mine, IL	J. S. White (Smithsonian Institution)	Single crystals #R 16603

Infrared spectra were measured in the mid-range (4000 to 300 cm^{-1}), using powders vacuum cold-pressed into KBr discs on a Perkin-Elmer model 621 spectrometer. Spectra in the far infrared were measured on powders mulled with mineral oil and smeared onto polyethylene plates. Spectra were measured from 33 to 700 cm^{-1} on a Beckman IR-11 spectrometer. The spectra presented in the figures from 800 to 4000 cm^{-1} are direct tracings from the Perkin-Elmer charts. Spectra below 800 cm^{-1} were replotted because of varying wavenumber scales on the Beckman spectrometer. It was shown (White, 1974a), by comparison of powder with single-crystal IR spectra, that the particle-size effects that render powder spectra of highly ionic materials almost invalid have only small effects on the IR spectra of carbonates. The wavenumber shift between the observed band and the true transverse mode frequency is largest for bands of high oscillator strength and is on the order of 10 to 20 cm^{-1} for the intense ν_3 (1400 cm^{-1}) mode of the carbonate ion. Sharp bands that appear in the IR spectra of the double carbonates are probably accurate to within 2 cm^{-1}, whereas the strong and broad bands are probably on the order of 10 to 20 wavenumbers higher than might be expected from single-crystal measurements.

Raman spectra were measured on a Spex model 1401 double monochromator using an RCA 200 mw argon ion laser as a source. The detector was a cooled RCA 31034 photomultiplier with photon-counting electronics. Spectra were measured using both 488 and 514.5 nm lines to check the authenticity of Raman bands and avoid luminescence problems. Spectral slit widths were typically 2 cm^{-1}, and the wavenumber accuracy is ± 3 cm^{-1}.

Results and discussion

Infrared and Raman spectra for all minerals studied are shown in Figures 2 through 7. In general, the spectra may be separated into two regions. Those bands at frequencies above 600 cm^{-1} are due to the internal motions of the molecular carbonate ion. Those below 600 cm^{-1} are due to motions involving the entire unit-cell (usually referred to as lattice modes in the spectroscopic literature).

The internal modes can be related to the vibrations of the free carbonate ion by simply comparing the band frequencies. Band frequencies for the free ion are listed in Table 3 along with the accepted assignments. The frequencies conventionally cited go back to Herzberg (1945), who in turn quoted the work of Kujumzelis (1938). These frequencies are compared in Table 3 with new measurements of the three Raman-active modes made on alkali carbonate (Na^+, K^+, and Rb^+) aqueous solutions. The agreement between the laser-excited spectra and the older Hg-

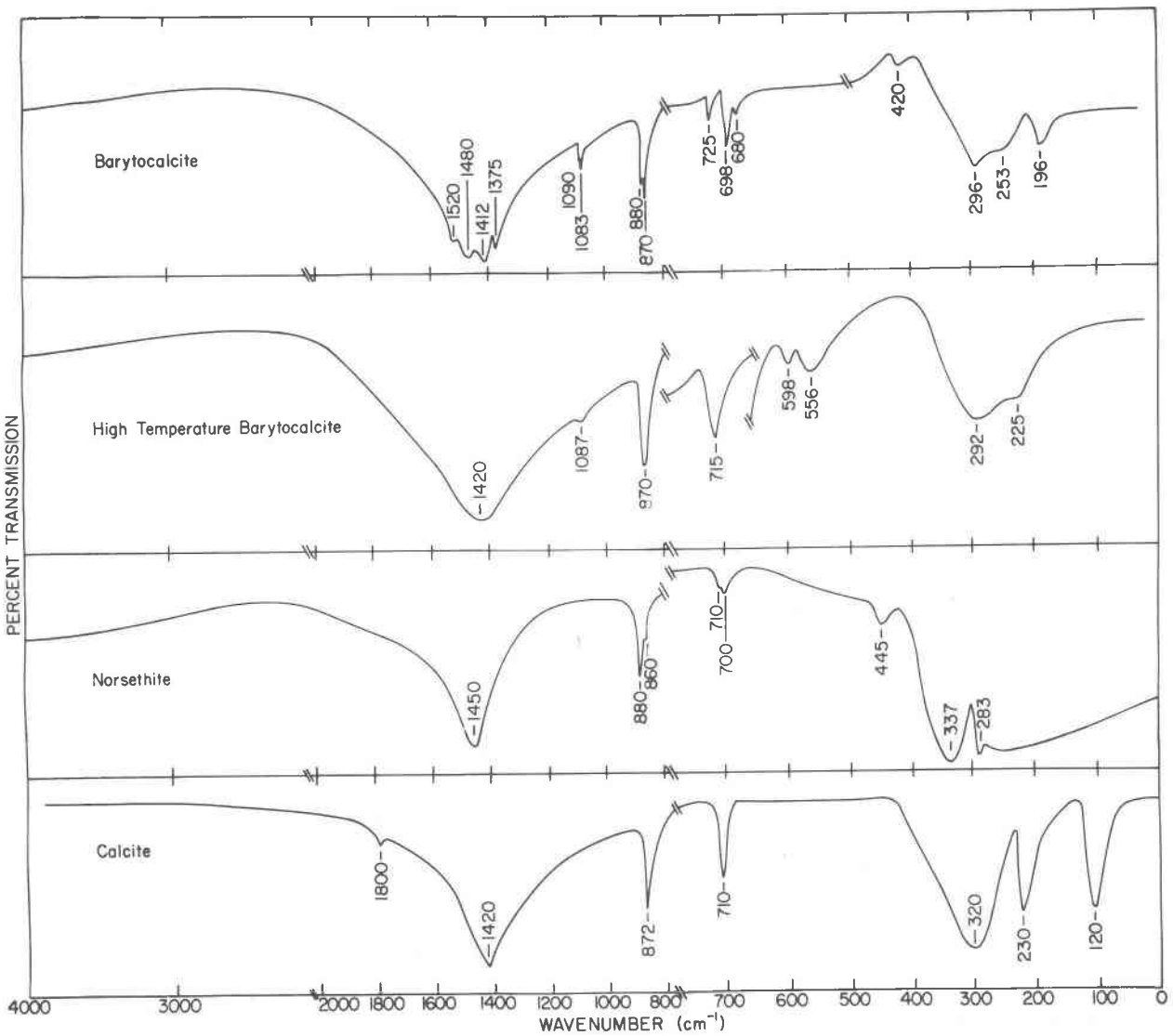

Fig. 2. Infrared spectra of barytocalcite, $CaBa(CO_3)_2$, the high-temperature modification of barytocalcite, and norsethite, $MgBa(CO_3)_2$, with the spectrum of calcite.

lamp-excited spectra is very good. There is some influence of the local environment on the frequencies, even in 1 M alkali carbonate solutions. The quoted value of ν_1 of 1064 cm^{-1} was observed in K_2CO_3 and Rb_2CO_3 solutions, whereas the frequency in Na_2CO_3 solution was 1069 cm^{-1}. The A_1 symmetric stretch is very intense in the Raman effect, while ν_3 and ν_4, although Raman-allowed, are extremely weak.

Minerals with ordering between cation layers

A factor-group analysis for norsethite is given in Table 4. The structure contains two CO_3^{2-} ions in the primitive cell, but these occupy equivalent sites with C_3 point symmetry. The trigonal symmetry of the carbonate site does not lift any of the degeneracy of the carbonate-ion vibrations, and there will be no site-group splitting. However, the presence of two ions in the non-centrosymmetric cell implies a factor-group splitting. The internal modes listed in the table are each duplicated, and the two components will have slightly different frequencies. The contrast in internal mode distribution of the non-centrosymmetric norsethite structure with the centrosymmetric dolomite structure is apparent. The center of symmetry separates the factor-group pairs of dolomite into separate IR and Raman-active sets which in norsethite factor-group pairs appear in the same spectrum.

The infrared spectrum of norsethite (Fig. 2) is in

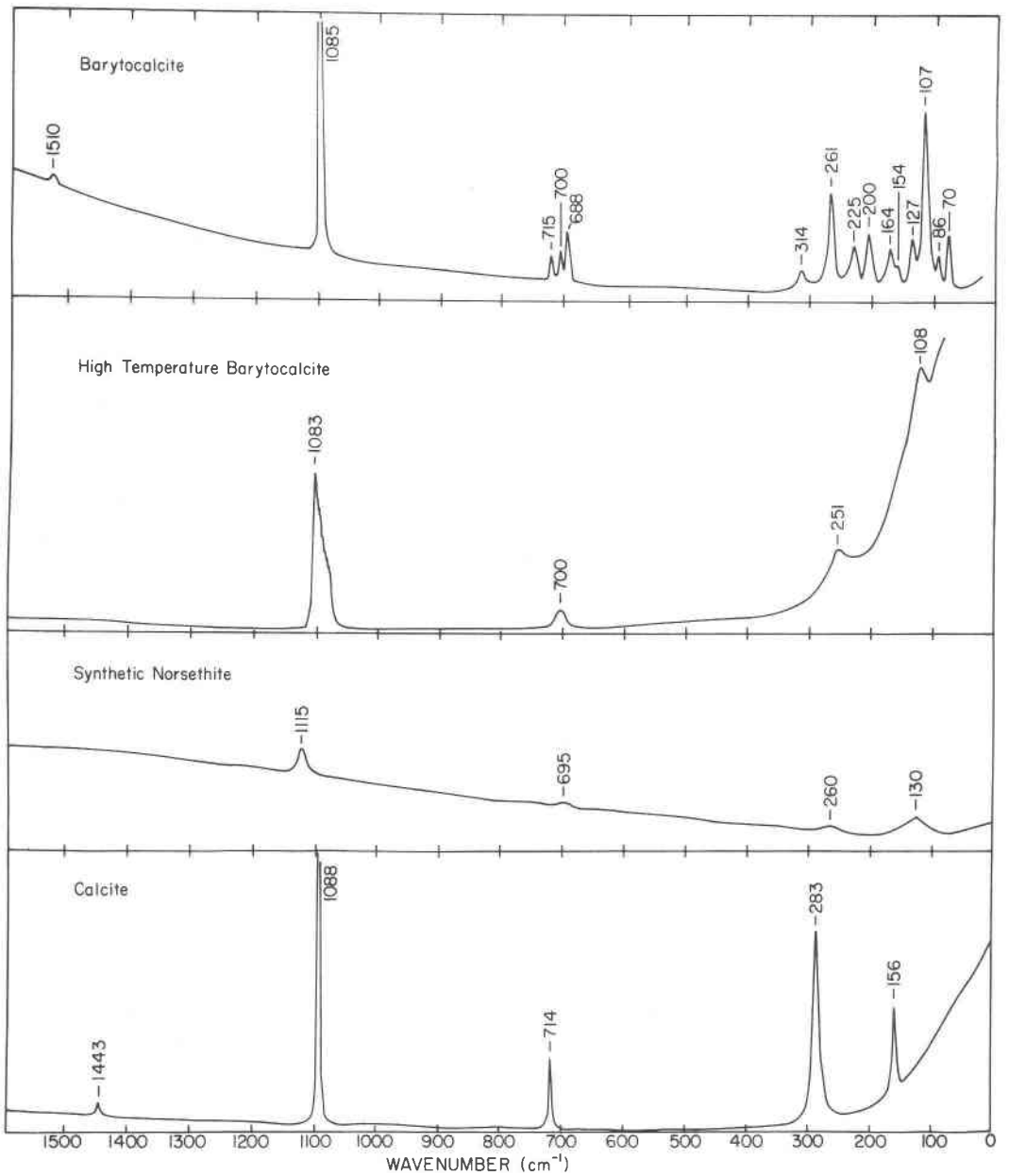

Fig. 3. Raman spectra of barytocalcite, $CaBa(CO_3)_2$, the high-temperature modification of barytocalcite, and norsethite, $MgBa(CO_3)_2$, with the Raman spectrum of calcite.

excellent agreement with these predictions. The selection rules in Table 4 show that ν_2, ν_3, and ν_4 are IR active. All three bands appear in the spectrum, and there is no evidence for the IR-forbidden ν_1. The bending modes ν_2 and ν_4 are each split into doublets separated by 10 cm^{-1} which may be taken as a measure of the factor-group splitting. The splitting is not resolved in the intense and broad ν_3 band.

The Raman spectrum of norsethite is very weak, and the bands are ill-defined (Fig. 3). Since this sample of norsethite was prepared by low-temperature precipitation, it is possible that the structure did not equilibrate into a well-ordered form, although the X-ray diffraction pattern showed sharp intense lines. The compound was prepared by several procedures, but all preparations gave the same spectrum as the one illustrated. A possible explanation would be poor translational ordering, which past experience (White

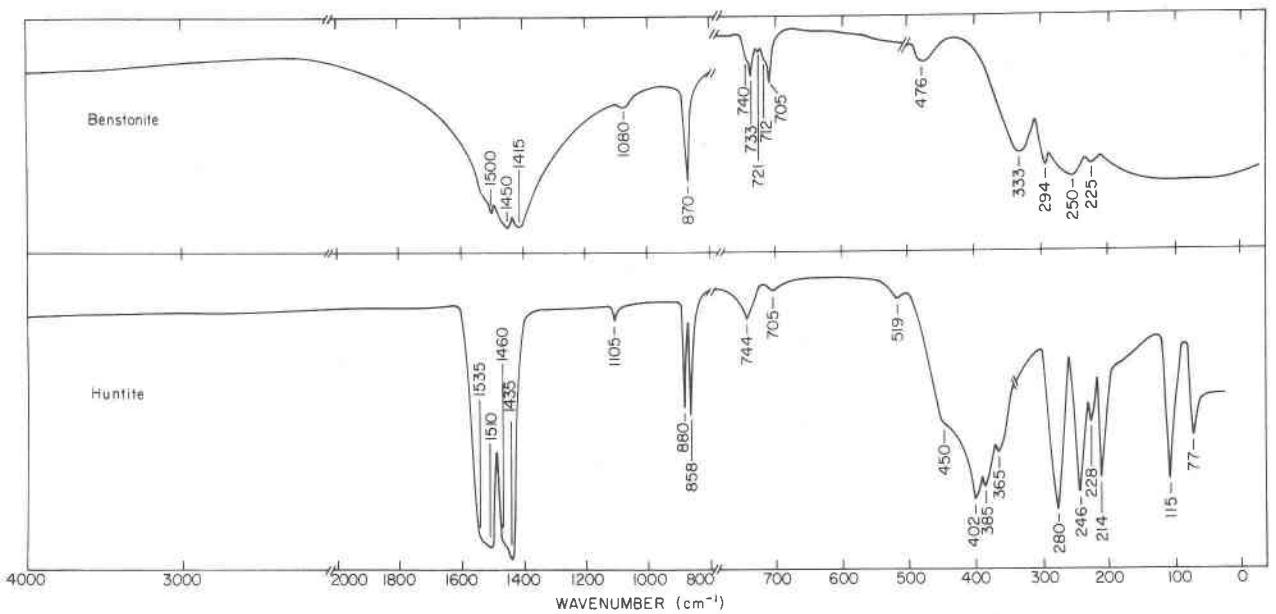

Fig. 4. Infrared spectra of benstonite, $Ca_7Ba_6(CO_3)_{13}$, and huntite, $CaMg_3(CO_3)_4$.

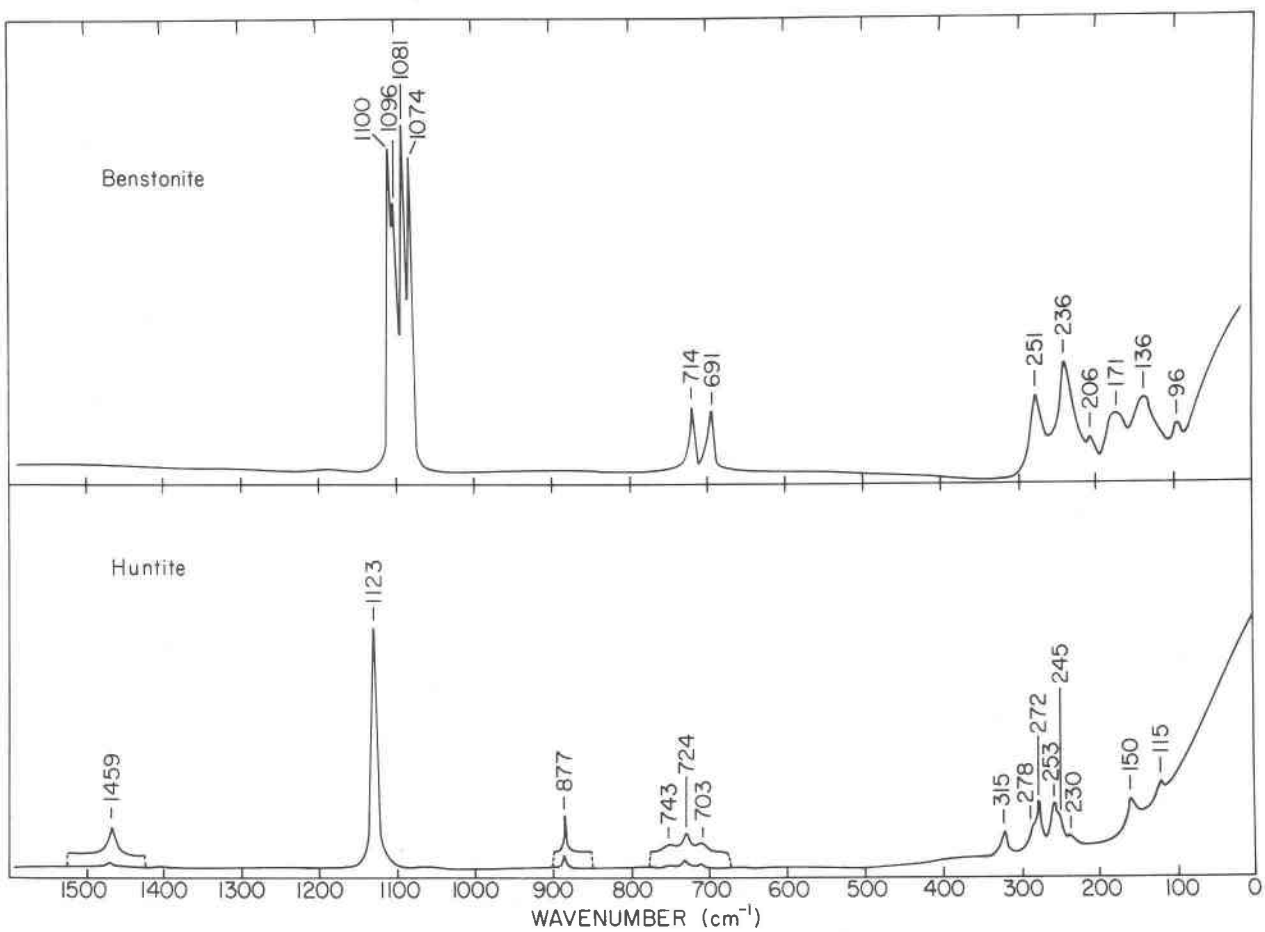

Fig. 5. Raman spectra of benstonite, $Ca_7Ba_6(CO_3)_{13}$, and huntite, $CaMg_3(CO_3)_4$.

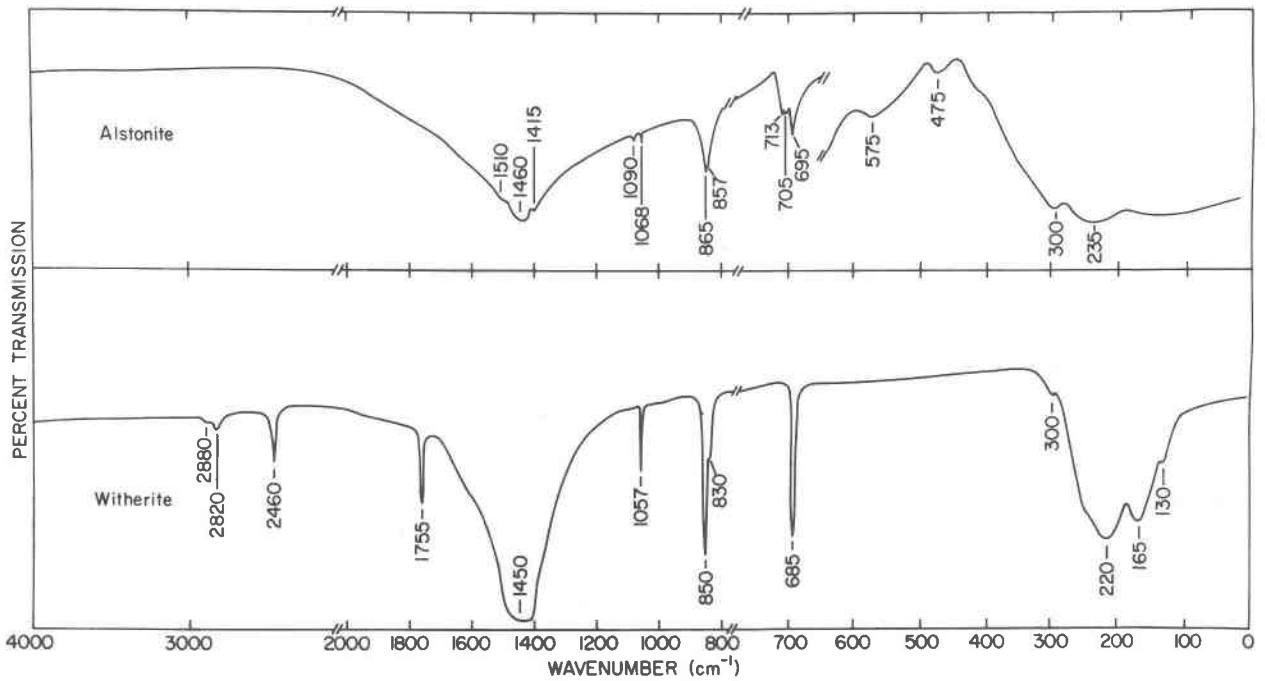

Fig. 6. Infrared spectrum of alstonite, $CaBa(CO_3)_2$, compared with the spectrum of witherite, $BaCO_3$.

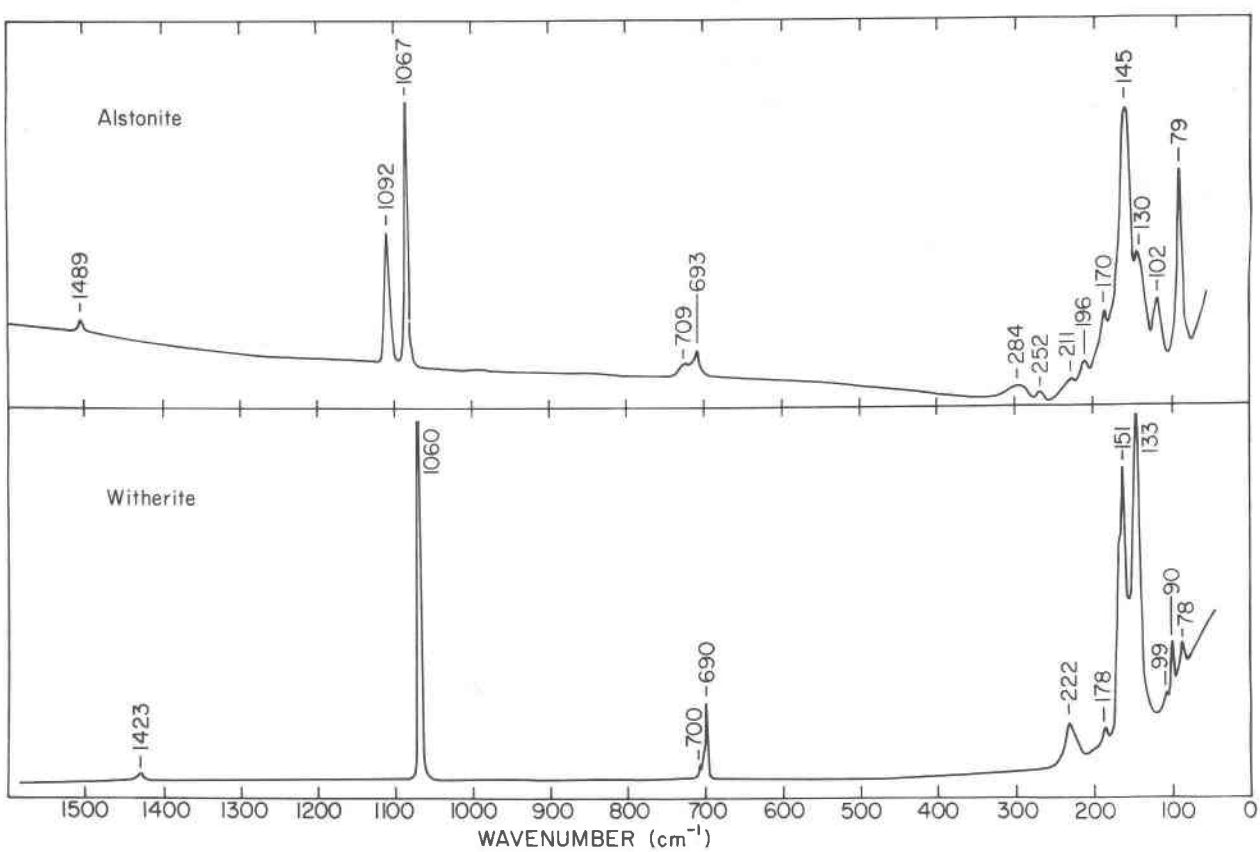

Fig. 7. Raman spectrum of alstonite, $CaBa(CO_3)_2$, compared with the spectrum of witherite, $BaCO_3$.

Table 3. Normal modes of the free carbonate ion

Mode*		Symmetry	Selection Rules	Frequency (cm^{-1}) Kujumzelis (1938)	This Work
ν_1	Symmetric stretch	A_1'	Raman	1063	1064
ν_2	Out-of-plane bend	A_2''	IR	879	-
ν_3	Asymmetric stretch	E'	IR + Raman	1415	1415
ν_4	In-plane bend	E'	IR + Raman	680	680

*Herzberg (1945) notation.

and Keramidas, 1972) shows to affect Raman intensities and line shapes more than the IR spectrum.

The band at 1115 cm^{-1} is the symmetric stretching frequency of the carbonate ion, which appears only in the Raman spectrum in the norsethite structure. However, ν_3, which should also be Raman active, is not observed, and ν_4 is very weak. The predicted factor-group splitting is not observed in either ν_1 or ν_4, although the very low intensity of the bands makes it difficult to assign a special significance to this.

Both IR and Raman spectra of norsethite have a strong resemblance to the spectra of calcite, which is shown in Figures 2 and 3 for comparison. This is especially true in the lattice vibration region where two weak bands in the Raman spectrum of norsethite at 260 and 130 cm^{-1} are similar to the corresponding 283 and 156 cm^{-1} bands of calcite. The factor-group analysis for the norsethite structure predicts 7 Raman-active lattice modes, but only these two are observed. Only three of a predicted eight lattice modes are observed in the infrared, and these have a certain superficial resemblance to the calcite spectrum. Detailed comparison is difficult because the lattice vibration region of the norsethite spectrum is masked by a broad absorption continuum of unknown origin.

The situation here is similar to the case of dolomite (White, 1974a), whose factor-group calculation is shown in Table 4 for comparison. The ordering of the cation layers in dolomite lowers the symmetry from $R\bar{3}c$ to $R\bar{3}$. The predicted effect on the spectrum is a relaxation in selection rules. The symmetric stretch, ν_1, is permitted in the IR, and ν_2 becomes permitted in

Table 4. Factor group analyses for norsethite and dolomite

	Total Modes	Acoustic Modes	Lattice Modes	Internal Modes	Selection Rules
D_3	NORSETHITE				
A_1	4	-	2	$2\nu_1$	Raman
A_2	6	z	3	$2\nu_2$	IR
E	10	(x,y)	5	$2\nu_3 + 2\nu_4$	IR + Raman
S_6	DOLOMITE				
A_g	4	-	2	$\nu_1 + \nu_2$	Raman
E_g	4	-	2	$\nu_3 + \nu_4$	Raman
A_u	6	z	3	$\nu_1 + \nu_2$	IR
E_u	6	(x,y)	3	$\nu_3 + \nu_4$	IR

Table 5. Normal modes and selection rules for barytocalcite

C_{2h}	Total Modes	Lattice Modes: Acoustic	Lattice Modes: Translational	Lattice Modes: Rotational	Internal Modes*: $CO_3(1)$	Internal Modes*: $CO_3(2)$	Selection Rules
A_g	18	-	8	2	$\nu_1 + \nu_2 + \nu_3' + \nu_4'$	$\nu_1 + \nu_2 + \nu_3' + \nu_4'$	Raman
B_g	12	-	4	4	$\nu_3'' + \nu_4''$	$\nu_3'' + \nu_4''$	Raman
A_u	12	z	3	4	$\nu_3'' + \nu_4''$	$\nu_3'' + \nu_4''$	IR
B_u	18	x,y	6	2	$\nu_1 + \nu_2 + \nu_3' + \nu_4'$	$\nu_1 + \nu_2 + \nu_3' + \nu_4'$	IR

*ν_3' and ν_3'' etc. label the corresponding site group components of the vibrational mode the degeneracy of which has been lifted by the non-trigonal site.

the Raman. A previously forbidden lattice mode appears in the IR, and two additional lattice modes appear in the Raman. In reality, none of these additional features are observed. The IR and Raman spectra of dolomite (White, 1974a) are essentially identical to those of calcite.

It may be concluded from this examination of the spectra that norsethite behaves dynamically very much like calcite and that the alternating Ba and Mg layers manifest themselves mostly in the factor-group splitting of the CO_3^{2-} bending modes.

A factor-group analysis is given for barytocalcite in Table 5. There are four CO_3^{2-} ions paired in two crystallographically distinct sites both with site symmetry C_s. Although the degeneracy of the CO_3^{2-} vibrations is lifted in an identical manner, because of the different local field around the two ions, the internal modes should appear as a superposition of two sets of bands. The space group for barytocalcite is centrosymmetric, and thus the factor-group components are separated into an IR-active set and a Raman-active set for each pair of CO_3^{2-} ions. The distribution of internal modes shown in Table 5 accounts for all degrees of freedom of the four CO_3^{2-} ions in the primitive unit-cell.

The infrared spectrum (Fig. 2) is in good agreement with the factor-group predictions. The strong band, ν_3, appears with four distinct components separated by a maximum of 145 cm^{-1}. This very large splitting is a combination of the differing crystal field around the distinct CO_3^{2-} ions and the distortion field around each ion. It is not possible, from powder data alone, to assign the bands separately to the two effects. The symmetric stretch, ν_1, appears in the spectrum because of the relaxed selection rules of the lower symmetry structure. This band appears as two components as does the symmetric band, ν_2. Both of these bands are non-degenerate in the free ion, so that the small splitting, 7 cm^{-1} for ν_1, and 10 cm^{-1} for ν_2, results because of a different symmetric component of the crystal field around the two carbonate sites. Band ν_4 is predicted to appear as four components; only three are observed. The IR spectrum of a barytocalcite from Cave-in-Rock, Illinois, published by Rossman and Squires (1974), does show a fourth weak band on the high-frequency side of the central peak. The lattice-mode region of the barytocalcite spectrum is not well resolved, with only four broad bands in a region where the calculation predicts 15 bands.

The Raman spectrum (Fig. 3) does not conform to predictions as well as the IR. The strong band at 1085 cm^{-1} does not show the expected splitting, although judging by the very small separation of the corresponding IR band, the splitting may be too small to resolve. Only a single component of ν_3 is observed where four are predicted. Band ν_4 shows only three of the expected four components, and band ν_2 does not appear at all. In the case of the bending modes, however, measurements of the Raman spectra of barytocalcite that had been heated through the phase transition and cooled again to room temperature do show a fourth component of ν_4 as a shoulder at 680 cm^{-1}, and ν_2 appears as a weak band at 875 cm^{-1}. The lattice-mode region shows ten distinct bands compared with the 18 predicted. The density of bands in this region is high, and it is not surprising that some bands in the powder spectrum would be overlapping and that weak bands would not be observed. Spectral measurements on oriented single crystals would be required to resolve further detail.

Barytocalcite undergoes a reversible phase transi-

Table 6. X-ray powder diffraction data for some double carbonates showing the relationship to calcite

Calcite		Norsethite			High Barytocalcite	
d(a)	hkl*	d(b)	hkl*	d(c)	d(c)	hkl*
	-	5.58	111	5.59	6.15	111
	-	4.21	100	4.20	4.35	100
3.86	110	3.86	110	3.86	3.99	110
	-		-	3.67		-
3.035	211	3.02	211	3.13	3.11	211
2.845	222	2.795	222			222
	-	2.656	221	2.660	2.786	221
2.495	$10\bar{1}$	2.512	$10\bar{1}$	2.507	2.599	$10\bar{1}$
2.285	210	2.290	210	2.292	2.215	210
	-	2.154	$11\bar{1}$	2.154	2.154	$11\bar{1}$
	-	2.104	322	2.104	1.966	322
2.095	200		-			-
1.927	220	1.931	220		1.943	220
1.913	332	1.890	332			332

(a) JCPDF #5-586 (b) JCPDF #12-530 (c) Synthetic, this work.

JCPDF = Joint Committee on Powder Diffraction Files

tion at 525°C (Chang, 1965). The transition is rapid enough to appear on a DTA trace but sluggish enough that the high-temperature form can be quenched for spectral measurements.

The IR spectrum of high-temperature barytocalcite bears a remarkable resemblance to the spectra of norsethite and calcite (Fig. 2). The only disagreement is the appearance of ν_1 as a very weak band at 1087 cm^{-1}. This band is forbidden on both the calcite and norsethite space groups. However, its appearance may be due to the presence of low-temperature barytocalcite formed during quench or on standing at room temperature. The correspondence in the Raman spectra is very good (Fig. 3). The symmetric stretching mode at 1083 cm^{-1} appears greatly broadened, as would be expected from a disordered structure.

The X-ray powder diffraction data for high-temperature barytocalcite can be indexed on the norsethite cell, which Lippman (1973) has previously shown to be a superstructure on calcite (Table 6).

In order for the monoclinic barytocalcite to transform to the rhombohedral norsethite-like structure, the carbonate groups are required to undergo two rotations. The $CO_3^{2-}(2)$ group would be first required to rotate 20° back into the plane parallel to the layering of the cations. Then both carbonate groups would need to rotate approximately 13° about the 3-fold axis to reach the correct positions for the norsethite structure.

The rotations of the carbonate groups would not be expected to be energetically favored at 525°C, and in fact the DTA trace indicates that the transition is rather sluggish. Raman spectra were measured as a function of temperature in a high-temperature cell to investigate this point (Figs. 8 and 9). Band ν_4 gradually blurs and loses detail as the temperature is increased to the phase transition, so that the transition itself produces only the final smoothing of this group of bands into a single broad peak. The lattice modes behave in much the same way, with the intermediate bands becoming weaker and losing detail, until at the phase transition, only the two strongest bands survive to become the two bands in the high-temperature phase that match the lattice modes of the norsethite structure. The reversibility of the transition appears clearly in the spectra, where the spectra of specimens that have been heated and then cooled to room temperature are, in fact, sharper and better resolved than the original material. The gradual broadening of the

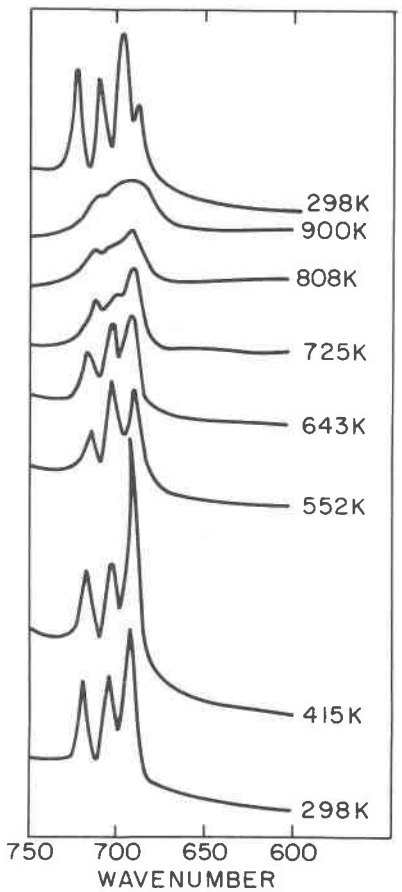

Fig. 8. Raman spectra of the ν_4 band of barytocalcite, $CaBa(CO_3)_2$ from *in situ* measurements at the indicated temperatures. The final spectrum taken on return of the cell to room temperature shows the increased order of the sample in terms of an improved resolution of this group of bending modes.

Raman lines at temperatures far below the transition temperature indicates that rotational disordering of the carbonate groups begins at lower temperatures and that the phase transition is only the final culmination of the disordering process.

Minerals with ordering within the cation layers

There are two crystallographically distinct carbonate ions in the huntite structure. $CO_3(1)$ lies in the basal plane of the trigonal cell and has point symmetry D_3, the same as the parent calcite. The remaining three $CO_3(2)$ ions are arranged around the three-fold axis and are inclined to the basal plane. All three are crystallographically equivalent with site symmetry C_2.

The vibrational behavior of huntite was analyzed by factor-group methods (White, 1974a), with the result shown in Table 7. The distribution of internal modes here is quite interesting. Since $CO_3(1)$ lies on a site of D_3 symmetry and is perpendicular to the c axis, the distribution and selection rules for the molecular modes are the same as for calcite. The remaining three CO_3^{2-} ions on sites of C_2 symmetry are tilted with respect to the c axis of the unit cell. Therefore, not only is the degeneracy of the vibrations lifted by the low site symmetry, but the modes are projected among both parallel and perpendicular factor-group representations. Since there are three molecules, there

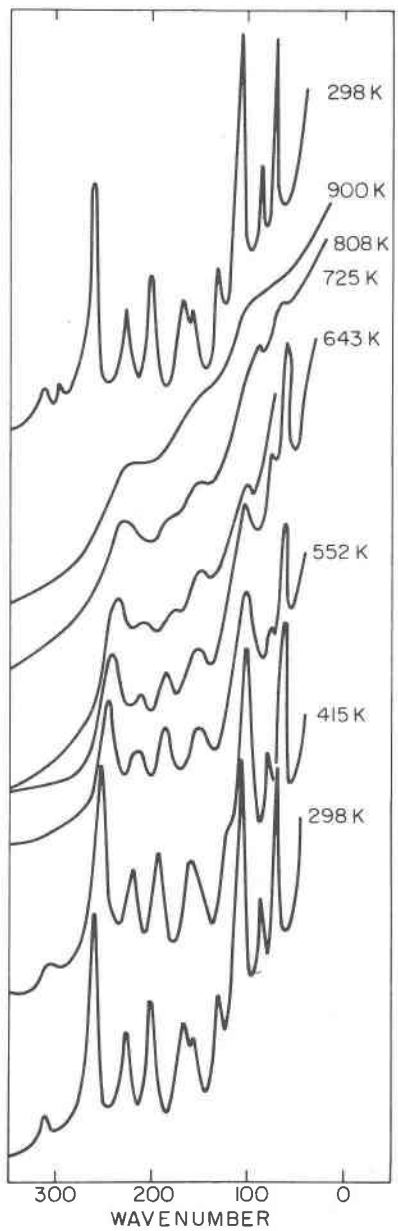

Fig. 9. Lattice modes of barytocalcite, $CaBa(CO_3)_2$ from *in situ* measurements at the indicated temperatures.

Table 7. Normal modes and selection rules for huntite

D_3	Total Modes	Lattice Modes: Acoustic	Lattice Modes: Translational	Lattice Modes: Rotational	Internal Modes*: $CO_3(1)$	Internal Modes*: $3CO_3(2)$	Selection Rules
A_1	7	-	2	1	ν_1	$\nu_1 + \nu_3' + \nu_4'$	Raman
A_2	13	z	5	3	ν_2	$\nu_2 + \nu_3'' + \nu_4''$	IR
						$\nu_1 + \nu_2 + \nu_3' +$	
E	20	(x,y)	7	4	$\nu_3 + \nu_4$	$\nu_3'' + \nu_4' + \nu_4''$	IR + Raman

*Primes and double primes refer to site group components.

are three ν_1 modes. One of these belongs to the A_1 representation of the factor group as expected. The remaining two, however, are combined by the factor group and fall into the degenerate E representation. ν_2 behaves similarly. The E' representation of ν_3 and ν_4 splits into $A + B$ on site group C_2. There are thus six components each of ν_3 and ν_4 to distribute among the representations of the factor group. The predicted spectrum, therefore, is a superposition of three effects: (1) The distinction between two crystallographically different carbonate ions will result in two independent internal-mode spectra with different frequencies and selection rules. (2) The low site-symmetry of the tilted CO_3^{2-} ions will result in a splitting of one set of ν_3 and ν_4 modes. (3) The correlation field will cause further separation and changes in selection rules of the second group of internal modes.

Vibrational spectra for huntite are shown in Figures 4 and 5. The specimens from Current Creek, Nevada, and Tea Creek, Australia, both gave essentially the same spectrum in which the lattice-mode region contained many sharp, well-defined bands. In contrast, the specimen from Wind Cave, South Dakota, produced a spectrum in which the lattice-mode region in the infrared was greatly broadened, and the only Raman band to appear was the intense ν_1 mode. The mid-range infrared bands of Figure 4 agree well with band positions previously reported by Adler and Kerr (1963).

A surprisingly complete, if tenuous, assignment can be made from powder spectra by carefully comparing IR and Raman coincidences with the predictions of the factor-group calculation. Assignments are summarized in Tables 8 and 9. Three bands arising from ν_1 are predicted, one due to $CO_3(1)$, one due to $CO_3(2)$ (both Raman-active), and an E-species component of ν_1 which is both IR- and Raman-active. The single weak band at 1105 cm^{-1} in the IR can then be immediately assigned to the E species component. Only one strong band appears at 1123 cm^{-1} in the Raman spectrum. It can be argued that, since correlation field coupling is relatively weak in all other carbonate spectra examined, the various band components that arise from the combinations of the three $CO_3(2)$ ions will have similar frequencies. Therefore, since the 1123 cm^{-1} Raman band is shifted substantially from the IR band, it is argued that this band arises from ν_1 of the unique $CO_3(1)$ and that the remaining component of ν_1 expected near 1105 cm^{-1} is too weak for observation in the Raman spectrum.

A similar argument applies to ν_2. Two components are expected to be only IR-active while a third component is both IR- and Raman-active. The single Raman-active band observed must therefore be the component of ν_2 belonging to the E species. Since the different components arising only from the correlation field splitting of ν_2 are expected to be of similar frequency, the 880 cm^{-1} IR band must be either the component of ν_2 from $CO_3(2)$ in the IR-active A_2 species, or the component in the E species, or both. This leaves the 858 cm^{-1} IR band to be assigned to ν_2 from $CO_3(1)$.

Four components of ν_3 are expected in the IR and four in the Raman, three of which should be coincident. The IR-active antisymmetric stretch is indeed split into four components, but only one weak band appears in this region in the Raman. The 1459 cm^{-1} Raman band is taken as coincident with the 1460 cm^{-1} IR band, and this pair is assigned to one of the E species components of ν_3. Furthermore, since $CO_3(1)$ has produced the strongest Raman bands for the other modes, this band is probably the component of ν_3 from $CO_3(1)$. Of the remaining three IR-active components of ν_3, two are of similar frequency and lie at much higher frequencies than the third. The doubly-degenerate ν_3 mode is split by the site crystal

Table 8. Assignments for internal modes of huntite

	$CO_3(1)$		$CO_3(2)$		
A_1		ν_1 1123(R)	ν_1 ?	ν_3' ?	ν_4' ?
A_2		ν_2 858(IR)	ν_2 880(IR)	ν_3'' 1535(IR) (?)	ν_4'' ?
E	ν_3 1459(R) 1460(IR)	ν_4 724(R)	ν_1 1105(IR)	ν_2 877(R)	ν_3' 1435(IR)
			ν_3'' 1510(IR) (?)	ν_4' 703(R) 705(IR) (?)	ν_4'' 743(R) 744(IR) (?)

field, and the usual observation has been that the crystal field splitting in carbonates is larger than the correlation field splitting. This would suggest that the similar 1510 and 1535 cm^{-1} bands represent the correlation field split pair (A_2 and E type) called ν_3'' in the factor-group analysis, while the remaining band at 1435 cm^{-1} is the ν_3' site-group component (E-type). This arrangement yields a site-group splitting of 88 cm^{-1} and a factor-group splitting of 25 cm^{-1}, which is at least consistent with many other observations in similar types of materials. It is not possible to determine which of the 1510 and 1535 cm^{-1} nodes belongs to A_2 and which to E on the basis of unpolarized powder spectra. Their listing (with "?") in Table 8 is arbitrary.

The assignments for ν_4 are more arbitrary, because only two components are observed in the IR although three appear in the Raman. The assignments listed in Table 8 have been made using the same sorts of arguments used for ν_3 except that there is a larger uncertainty.

Table 9. Assignments for lattice modes of huntite

Observed	$A_1(R)$	$A_2(IR)$	E	
			R	IR
	315	519	278	280
	272	450	245	246
	253	402	230	228
	150	385	115	115
		365		
		214		
		77		
Predicted	3	8	11	

Classification of the lattice modes into the three irreducible representations of D_3 are made in Table 9 on the basis of coincidences between the IR and Raman spectra. The numbers at the bottom of the table list the number of modes predicted by factor-group analysis. The presence of an extra band of the A_1 type must mean that at least one of them has an unobserved IR component, since only 4 of the 11 predicted E type modes were observed.

Very little is known about the structure of benstonite other than its space group and the fact that there are 13 carbonate ions in the unit cell. The exact cation content of the cell and the cation arrangement are uncertain (Lippmann, 1973). Infrared spectra (Fig. 4) and Raman spectra (Fig. 5) may be compared with spectra of the other carbonates. The IR spectrum would be consistent with a derivative of calcite with the $R3$ space group. At least three components of ν_3 and 5 components of ν_4 are observed. However, only one component of ν_1 and ν_2 appear. The Raman spectrum is quite remarkable, since at least four distinct components of ν_1 appear with high intensity. This would suggest at least four crystallographically distinct CO_3^{2-} ions, since the minerals previously discussed show that the correlation field is rarely strong enough to produce a multiplicity in ν_1. Factor group C_3 has only two irreducible representations A and E, which are both IR- and Raman-active, so there are no selection rules applicable to powders. The strongest component of the ν_1 Raman modes appears to be coincident with the very weak ν_1 band in the IR. In contrast, the ν_3 bands which are the strongest bands in the IR do not appear in the Ra-

man at all. The near exclusion suggests that the benstonite structure must on the average be nearly centrosymmetric in spite of its non-centrosymmetric space group, as might be expected from a calcite superstructure. Benstonite does not yield any evidence for second harmonic generation, which supports the above conclusion.

Aragonite-related minerals

The structure of alstonite is unknown except for the space group, on the basis of which it has been claimed that alstonite is related to aragonite rather than forming a derivative structure of calcite as the minerals previously discussed. IR and Raman spectra for alstonite are shown in comparison with witherite in Figures 6 and 7. The IR spectrum of alstonite agrees fairly well with the mid-range results of Adler and Kerr (1963) and with the full IR spectrum of Rossman and Squires (1974).

Most interesting is the ν_1 mode, which appears as two distinct bands in the Raman. These modes also appear as very weak bands in the IR. This result suggests that there are two crystallographically-distinct carbonate ions in alstonite. One of these is partially disordered, which gives rise to the broadened symmetric stretching band. The half-width of the 1092 band is 10 cm^{-1} compared with 5 cm^{-1} for the 1067 band. In all simple-structure carbonates the half-width of ν_1 is in the range of one to five cm^{-1}. For example Park (1966) shows that ν_1 in calcite has a half-width of 1.1 cm^{-1} at 300 K.

Comparison of the lattice-vibration region of alstonite with that of witherite supports the hypothesis that alstonite is an aragonite-related structure. It is not isomorphous, because of the two distinct CO_3^{2-} groups, but the similarity of the lattice modes suggests that the overall structures are very similar.

Comparison of the alstonite spectra with the spectra of benstonite provides no support for the suggestion (Chang, 1965) that alstonite may be a Sr-stabilized calcite superstructure just as benstonite is a Mg-stabilized calcite superstructure.

Spectroscopic characterization of structural order

Most of the compounds examined in this paper can be regarded as derivatives of calcite. There are an enlarged number of formula units per primitive cell, reduced space-group symmetry due to ordering of cations, and rearrangements of the carbonate ions. Since the more complex structures contain both cations and anions on more than one equipoint, the possibility for disorder from the ideal structural arrangement is possible. The consequences of structural ordering and development of supercells can be calculated by factor-group methods as described in earlier publications (White, 1966; 1974b; White and Keramidas, 1972). Predicted changes in the vibrational spectra arise from:

(1) Composite spectra resulting from CO_3^{2-} ions being located on non-equivalent sites and therefore subject to different local fields.

(2) Band multiplicity due to correlation field (factor-group) interaction between CO_3^{2-} ions on equivalent sites.

(3) Relaxation of selection rules due to lower rotational symmetry of derivative space groups.

(4) Band splitting due to non-trigonal crystal fields (site-group splitting). Mode distributions and their selection rules are group theoretical results and only distinguish permitted interactions from forbidden interactions. Whether a predicted mode splitting will be large enough to observe will depend on the strength of the perturbation field responsible for the splitting and must be observed experimentally. Likewise whether a band permitted by the relaxation of selection rules will have an intensity large enough to measure above noise background will be determined by the dipole derivative or polarizability derivative created by the small changes in atomic position in the derivative structures.

Comparison of the spectra of the double-carbonate minerals suggests that the effects (1) and (4) are largest (in the range of 20 to 100 cm^{-1}) and are usually observed when predicted. Some splittings appear to be too small to revolve. Factor-group splittings are smaller, on the order of a few to perhaps 20 cm^{-1}. Selection-rule relaxations are not effective, as seen in the case of dolomite, norsethite, and other minerals. Bands predicted to appear in the IR or Raman from the relaxation of selection rules are seldom observed.

It appears that the small effects that arise from changes in rotational symmetry are best observed in the IR for the carbonate compounds. In most of the examples given, the predicted peak splitting and appearance of new bands was observed. In contrast, the Raman spectra frequently contained fewer bands than predicted. Extra bands and band splittings were not observed. Infrared band intensities are proportional to the derivative of the dipole moment with respect to the normal coordinate that describes the particular mode. Raman intensities are proportional to the derivative of the polarizability with respect to the appropriate normal coordinate. The couplings between various parts of the crystal that generate the

band multiplicities and splittings are dipolar in character and therefore likely to lead to larger changes in the dipole derivatives than in the polarizability derivatives.

Disorder in the arrangement of carbonate ions in the crystals is not described by group theoretical calculations. In structures such as the high-temperature form of barytocalcite and in alstonite it takes the form of a certain degree of randomness in the orientation of the carbonate ions. This is a form of intermediate range disorder which does not modify the nearest-neighbor environment very much and if anything would raise the overall symmetry of the structures. There is a partial breakdown in the translational symmetry of the structures which other work (see review by White, 1974b) shows to manifest itself as a line broadening. Infrared spectra of powders are already broadened by particle-size effects and lineshape comparisons are not reliable. Translational disorder does produce a marked broadening of the Raman lines, particularly the totally symmetric stretching mode. Other work from this laboratory (Brawer, 1975) shows that line broadening can be directly related to average translational order and can even be used as a tool to characterize the intermediate-range order in glasses. Observations of line shape permit the argument that the high-temperature form of barytocalcite is a disordered structure related to norsethite, and that one of the carbonate ions in the alstonite structure is on a somewhat disordered position.

Acknowledgments

We are grateful to Dr. D. L. Graf, University of Illinois, Dr. L. L. Y. Chang, Miami University, Dr. R. W. Grant, Lafayette College, and Dr. J. S. White, Jr., Smithsonian Institution, for specimens of carbonate minerals. This work was supported by the National Science Foundation under Grant No. EAR73-00243 A01.

References

Adler, H. H. and P. F. Kerr (1963) Infrared spectra, symmetry and structure relations of some carbonate minerals. *Am. Mineral., 48,* 839–853.

Alm, K. F. (1960) The crystal structure of barytocalcite, $BaCa(CO_3)_2$, *Arkiv. Mineral. Geol., 2,* 399–410.

Brawer, S. (1975) Theory of the vibrational spectra of some network and molecular glasses. *Phys. Rev., B 11,* 3173–3194.

Chang, L. L. Y. (1965) Subsolidus phase relations in the systems $BaCO_3$–$SrCO_3$, $SrCO_3$–$CaCO_3$, and $BaCO_3$–$CaCO_3$. *J. Geol., 73,* 346–368.

Dickens, B. and J. S. Bowen (1971) The crystal structure of $BaCa(CO_3)_2$ (barytocalcite). *J. Res. Natl. Bur. Stand., 75A,* 197–203.

Graf, D. L. (1961) Crystallographic tables for the rhombohedral carbonates. *Am. Mineral., 46,* 1283–1316.

——— and W. F. Bradley (1962). The crystal structure of huntite, $Mg_3Ca(CO_3)_4$. *Acta Crystallogr., 15,* 238–242.

Herzberg, G. (1945) *Infrared and Raman Spectra of Polyatomic Molecules.* D. Van Nostrand, New York, 632 p.

Hood, W. C. and P. F. Steidl (1973) Synthesis of benstonite at room temperature. *Am. Mineral., 58,* 341–342.

Kujumzelis, T. G. (1938) Über die Schwingungen und die Struktur der XO_3-Ionen, *Z. Physik, 109,* 586–597.

Lippmann, F. (1973) *Sedimentary Carbonate Minerals.* Springer-Verlag, Berlin, 228 p.

Mrose, M. E., E. C. T. Chao, J. J. Fahey and C. Milton (1961) Norsethite, $BaMg(CO_3)_2$, a new mineral from the Green River Formation, Wyoming. *Am. Mineral., 46,* 420–429.

Park, K. (1966) New width data on the A_{1g} Raman line in calcite. *Phys. Lett., 22,* 39–41.

Rossman, G. R. and R. L. Squires (1974) The occurrence of alstonite at Cave-in-Rock, Illinois. *Mineral. Record., 5,* 266–269.

Rutt, H. N. and J. H. Nicola (1974) Raman spectra of carbonates of calcite structure. *J. Phys. C: Solid State Phys., 7,* 4522–4528.

Sartori, F. (1975) New data on alstonite. *Lithos, 8,* 199–207.

White, W. B. (1966) Application of infrared spectroscopy to order–disorder problems in simple ionic solids. *Mater. Res. Bull., 2,* 381–394.

——— (1974a) The Carbonate Minerals. Chapter 12 in, V. C. Farmer, Ed., *The Infrared Spectra of Minerals.* Mineral. Soc. London, 227–284.

——— (1974b) Order–disorder effects. Chapter 6 in, V. C. Farmer, Ed., *The Infrared Spectra of Minerals.* Mineral. Soc. London, 87–110.

——— and V. G. Keramidas (1972) Applications of infrared and Raman spectroscopy to the characterization of order–disorder in high temperature oxides. *Natl. Bur. Stand. Spec. Pub., 364,* 113–126.

Yamamoto, A., T. Utida, H. Murata and Y. Shiro (1975) Optically active vibrations and effective charges of dolomite. *Spectrochim. Acta, 31A,* 1265–1270.

Manuscript received May 21, 1976; accepted for publication, September 22, 1976.